

Risk and Resilience Assessment With Component Criticality Ranking of Electric Power Systems Subject to Earthquakes

Sebastián Espinoza ^{ID}, Member, IEEE, Alan Poulos ^{ID}, Hugh Rudnick ^{ID}, Fellow, IEEE, Juan Carlos de la Llera ^{ID}, Mathaios Panteli ^{ID}, Senior Member, IEEE, and Pierluigi Mancarella ^{ID}, Senior Member, IEEE

Abstract—Countries around the world suffer the dramatic impact of earthquakes and other natural hazards reflected in casualties, infrastructure damage, service interruptions, and recovery costs. Although disaster exposure consciousness of electric power systems has increased in recent years, mitigation and adaptation actions, such as reserve scheduling and infrastructure investments, are usually performed without quantitative tools to account for the underlying stochasticity of these events. This article first discusses why an integrated assessment, which incorporates sources of uncertainty (risk) and manages the time-dependency of the recovery process (resilience), should be used to assess the impact of seismic events on electric power systems. Thereafter, a probabilistic methodology that considers the hazard, vulnerability, operation, and recovery of the system is presented. As a case study, the probabilistic seismic resilience of the electric power system of Northern Chile is assessed using different risk measures, including expected annual loss, value at risk, and conditional value-at-risk. Finally, a novel criticality assessment based on these metrics is developed to demonstrate that, for certain networks such as the study case, retrofit of selective components can notably improve the resilience of the complete system to seismic events. For example, if one specific component from the 152 components of the study system is assumed invulnerable, expected annual interruption costs decrease by 8%.

Index Terms—Criticality ranking, earthquake response, economic impacts, importance measures, reliability, resilience, seismic risk assessment.

Manuscript received March 2, 2019; revised September 23, 2019; accepted November 23, 2019. Date of publication February 14, 2020; date of current version June 3, 2020. This work was developed within the Chile-UK Newton-Picarte Project for “Disaster Management and Resilience in Electric Power Systems” (Consortium that includes Pontificia Universidad Católica de Chile (PUC), Universidad de Chile (UCH), and The University of Manchester (UoM), U.K.), which is supported in part by CONICYT, Chile, and RCUK/EPSRC, U.K., under Grant EP/N034899/1, in part by Fondecyt under Grants 1170836, 1141082, and 1181136, in part by Fondecyt under Grant 15110017, and in part by U.K. EPSRC RESNET under Grant EP/I035781/1. (*Corresponding author:* Sebastián Espinoza.)

S. Espinoza is with the Pontificia Universidad Católica de Chile, Santiago 7820436, Chile (e-mail: sebaesp@puc.cl).

A. Poulos and J. C. de la Llera are with the Pontificia Universidad Católica de Chile, Santiago 7820436, Chile, and also with the National Research Center for Integrated Natural Disasters Management (CIGIDEN), CONICYT/FONDAP/15110017, Santiago 4860, Chile (e-mail: ajpoulos@uc.cl; jllera@ing.puc.cl).

H. Rudnick is with the Pontificia Universidad Católica de Chile, Santiago 7820436, Chile (e-mail: hrudnick@ing.puc.cl).

M. Panteli is with the University of Manchester, Manchester M13 9PL, U.K. (e-mail: mathaios.panteli@manchester.ac.uk).

P. Mancarella is with the University of Manchester, Manchester M13 9PL, U.K., and also with the University of Melbourne, Melbourne, VIC 3010, Australia (e-mail: p.mancarella@manchester.ac.uk).

Digital Object Identifier 10.1109/JST.2019.2961356

NOMENCLATURE

Constants

\bar{P}_g	Maximum output of generator g [MW].
$\bar{f}_l^{\mathcal{N}_1(l), \mathcal{N}_2(l)}$	Rating of circuit (which goes from node $\mathcal{N}_1(l)$ to node $\mathcal{N}_2(l)$) [MW].
π_g	Energy variable cost of generator g [US\$/MWh].
M	Sufficiently large auxiliary positive constant [US\$/MWh].
x_l	Reactance of circuit [pu].
S_0	Base apparent power [MVA].
D_k	Demand at node k [MW].
VoLL_k^t	Value of lost load at node k at hour t [US\$/MWh].
u_g^t	Status of generator g at time t due to outage, unit commitment, under construction, maintenance, island black-start capabilities, and/or start-up time required; value 1 if available, 0 otherwise.
u_l^t	Status of circuit at time t due to outage; value 1 if available, 0 otherwise.

Variables

P_g	Output of generator g [MW].
LS_k	Load shed at node k [MW].
$f_l^{\mathcal{N}_1(l), \mathcal{N}_2(l)}$	Power flow in circuit (which goes from node $\mathcal{N}_1(l)$ to node $\mathcal{N}_2(l)$) [MW].
θ_k	Voltage angle at node k [radians].
ENS_s	Energy not supplied in scenario s [MWh].
IC_s	Interruption cost in scenario s [US\$].

Sets

\mathcal{G}	Set of generators.
$\mathcal{G}(k)$	Set of generators connected to node k .
\mathcal{N}	Set of nodes.
\mathcal{L}	Set of circuits.
$\mathcal{N}_1(l)$	First (or “from”) end node of circuit l .
$\mathcal{N}_2(l)$	Second (or “to”) end node of circuit l .
\mathcal{T}	Set of hours running from 1 (event time of occurrence) until the system infrastructure is completely recovered.
\mathcal{S}	Set of scenarios.

Risk Measures

EAL	Expected annual loss.
VaR ^z (α)	Value at risk with an α -probability considering a time window of z years.
CVaR ^z (α)	Conditional value-at-risk with an α -probability considering a time window of z years.

Remark: When augmented with the superscripts “s” and/or “t,” the above variables or parameters represent their value at the scenario s and/or at time t after the seismic event has occurred.

I. INTRODUCTION

OUR world is increasingly threatened by catastrophic natural disaster risk, which is, moreover, disproportionately concentrated in low-income regions with weak governance [1], [2]. This is particularly relevant for countries located in the Pacific Ring of Fire, which, given their geological and geographical characteristics, are especially exposed to seismic risk that leads to high economic losses. Due to the high-impact and low-probability (HILP) nature of this type of events, it is fundamental to consider not only average indicators but also suitable HILP indicators. For example, in average, between 1980 and 2011, Chile registered losses quantified as 1.2% of its gross domestic product (GDP) every year due to natural hazards [1]. However, the earthquake and tsunami of 2010 alone produced losses of US\$30 000 million or 18% of Chile’s GDP [3].

Modern societies rely heavily on electricity, especially under a crisis; therefore, studying the seismic impact on electric power systems is of paramount importance. Nevertheless, any assessment of these impacts needs to deal with various sources of uncertainty, such as when will a future earthquake strike? What will be its magnitude? Where will its epicenter be located? What will be the damage on electrical components? How will the system recover? Given the stochastic nature of these events and the response of critical infrastructure, suitable probabilistic models are required to better characterize them and propose adequate mitigation and adaptation strategies within a formal risk analysis framework. Risk is meant here as the measurement of the probability and severity of unwanted negative events [4].

Risk analysis literature on electric power systems has probabilistically addressed the improvement on reliability by focusing on credible contingencies and average indicators (e.g., [5]–[12]). Recently, some authors have started to study how to enhance transmission and generation expansion planning when these systems face the occurrence of rare, high-impact events, such as seismic events [13]; however, the low number of scenarios and simplifications considered is not enough to appropriately model the necessary uncertainties as discussed in the present article. Furthermore, risk-based literature (e.g., [14]–[16]) has studied direct earthquake impacts on electric power systems, albeit it has not considered the postdisaster operational and infrastructure evolution.

When studying the impact of natural hazards, several types of analyses may be performed [17]. As the economic impact on critical infrastructure depends on different stages of the disaster

process, namely, hazard intensity and recurrence, system vulnerability, operational capabilities, and restoration protocols, a time-dependent analysis is required. These stages align with the concept of resilience, which refers to the ability of a system to adapt to changing conditions and withstand and recover rapidly from disruptions [18]–[22].

Resilience-based literature on earthquake impacts on electric power systems has not used so far a fully probabilistic risk framework (e.g., [23]), with some works using arbitrary earthquake scenarios with precalculated recurrence rates to assess the risk of the network (e.g., [24]). Even in the presence of an ideal resilience model to quantify the impact of a preselected disaster scenario, a crucial obstacle would still be what scenario to select and what kind of decisions can be made based on the information of a single or limited number of arbitrary scenarios. Therefore, a global and integrated assessment of risk and resilience to assess the impact of future earthquakes on electric power systems and that considers the combination of all possible scenarios is vital and still pending.

An important issue when performing risk and resilience based analyses is that, on the one hand, they are complex and use an enormous number of parameters and assumptions, and on the other hand, the results are hard to communicate to a broad audience. Since the system performance depends on its components, ranking components by their quantitative relative importance, as initiated by [25], is a convenient method to deal with the previous issues. Therefore, a criticality analysis can be a key tool to infer conclusions with assumptions and parameters under *ceteris paribus* conditions and become a useful tool to communicate to engineers and nonengineers which components are more critical, and thus what activities to prioritize, identify weak-links, improve expansion planning, and optimize restoration protocols, amongst others. Several authors have studied multifailure component criticality in electric power systems (e.g., [16], [26]–[30]). However, they neither consider risk nor resilience [26], whereas others are only resilience-based [27]–[30] or only risk-based [16] studies.

A research gap identified in previously cited literature related to the seismic impact on electric power systems, and in general when quantifying the impact of natural hazards on critical systems, is the absence of methodologies that result in outcomes that may be used by planners and policymakers to support cost-benefit analyses. This is because current methodologies either evaluate impacts of deterministic scenarios disregarding the probabilistic nature of the studied events (thus being “nonrisk” methodologies) or quantify the impact of the studied events disregarding the postdisaster operation and/or restoration of the system (hence being “nonresilience” methodologies). Furthermore, there are no risk and resilience studies that propose a consistent component criticality assessment.

To address the above research gaps, this article develops a novel risk and resilience-based component criticality assessment methodology of electric power systems under earthquake-induced failures. The criticality of components is computed using several risk measures, some of which are average indicators, represented here by the EAL, and others are HILP indicators, which focus on the tail of the loss probability distribution and

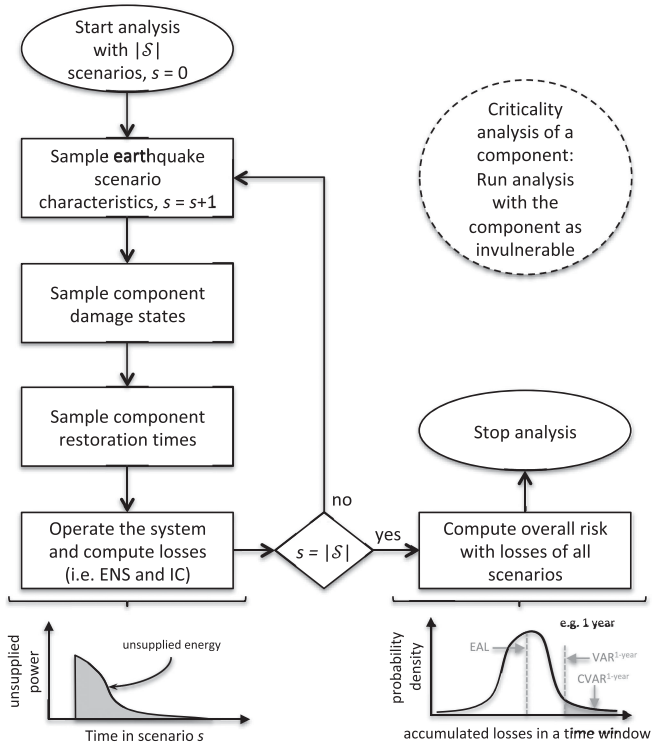


Fig. 1. Methodological flowchart for risk, resilience, and criticality analysis.

are represented here by the VaR and CVaR. The methodology presented, which can be extended to other natural disasters and critical infrastructure, is exemplified with the electric power system of Northern Chile, one of the most seismic prone regions in the world.

Finally, typical assumptions used by importance measures that have subtle but concrete differences on criteria and viewpoints, as reviewed by [31], are improved in this article, specifically regarding six areas mentioned hereafter. The importance measures presented here are based on: 1) risk analysis (opposed to conditional probabilities or deterministic scenarios); 2) simulation; 3) continuous performance system assessment (opposed to binary system states of functional or nonfunctional); 4) statistically dependent component failures due to common cause failures; 5) multistate component damage states; and 6) repairable components.

II. RISK, RESILIENCE, AND COMPONENT CRITICALITY QUANTIFICATION METHODOLOGY

A methodology coherent with the previously presented definitions of resilience, risk, and component criticality is summarized in Fig. 1 and explained in detail in the following subsections A, B, and C.

The methodology incorporates the two main contributions of this article. First, provide a novel global and integrated assessment of risk and resilience to assess the impact of earthquakes on electric power systems (which is described in detail in the two subsections “A. Resilience quantification” and “B. Risk quantification and uncertainty management”). Second, provide

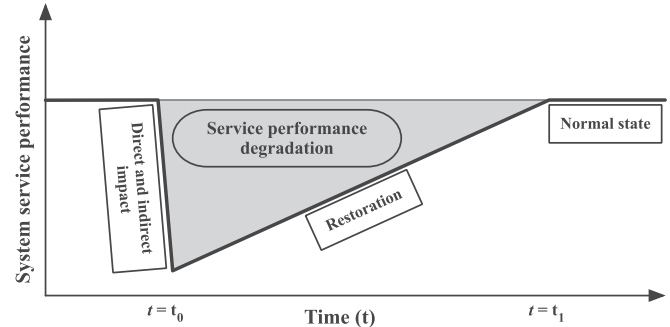


Fig. 2. Conceptual resilience curve (adapted from [18]–[22]).

a novel component criticality analysis with importance measures (which is described in detail in the third subsection “C. Criticality assessment”).

Fig. 1 depicts the main steps of the methodology in a flowchart that begins by defining an $|S|$ number of scenarios to be run, starting by scenario $s = 0$. Then, an earthquake scenario characterization is sampled and the scenario counter s is increased by one. Peak ground accelerations are used to determine the damage states of each component of the system based on a component vulnerability analysis. Thereafter, based on the damage, the component restoration times are sampled to define the complete recovery of the system. With this information, the system operation and response are simulated and the losses in terms of ENS and IC are computed for the particular scenario s .

The previous procedure is repeated for every scenario until the counter s reaches the total number of scenarios $|S|$. Then, using the results and frequencies of occurrence of all scenarios, the overall risk in terms of accumulated losses in a time window is computed.

Finally, for the component criticality analysis, the resilience and risk assessment summarized in the flowchart is repeated with one of the components treated as invulnerable to the hazard under analysis.

A. Resilience Quantification

Resilience may be described and quantified as a time-dependent process comprised of several stages [18]–[22]. Fig. 2 shows a conceptual resilience curve (also known as “resilience triangle”) to describe the time-dependent process under analysis and the use of service degradation as the main loss indicator for each scenario. In reality, however, the system response and recovery are not necessarily linear since they are affected by several factors as detailed later in this section.

In the case of the present article, the event impact is comprised of only one main shock that lasts from seconds to a few minutes; aftershocks and tsunami effects are not included. At time t_0 , the event causes direct and indirect impacts. Direct impact refers to structural damage, whereas indirect impact to electrical cascading damage, which is not considered here. After the system dynamically stabilizes, which is considered instantaneous here, the recovery stage between t_0 and t_1 may start with the deployment of repair crews and restoration of components until the system has recovered to a state equivalent to

the one before t_0 . In the present article, resilience quantification is methodologically described by the stages further explained in the next four subsections.

End users are not interested in the power system infrastructure itself, i.e., how many generators or substations were damaged, albeit they are primarily concerned with the unserved energy and corresponding service interruption cost. Consequently, for each scenario s , the system service performance metrics used are ENS, described in (1) as the sum across time of LS across all system nodes, and IC, described in (2) as the sum of LS valued at their respective nodal VoLL. The constant Δt represents the time step of the simulation (in our case one hour). Other costs, such as infrastructure damage and recovery costs, could also be included as natural extensions as follows:

$$\text{ENS}_s = \sum_{t \in \tau} \sum_{k \in \mathcal{N}} \text{LS}_k^{s,t} \times \Delta t \quad (1)$$

$$\text{IC}_s = \sum_{t \in \tau} \sum_{k \in \mathcal{N}} (\text{LS}_k^{s,t} \times \Delta t \times \text{VoLL}_k^t). \quad (2)$$

1) Stage 1. Hazard Characterization: The first stage consists in understanding the local hazard and building representative seismic scenarios. These scenarios are defined by a sampled time of occurrence and sampled earthquake intensities at the location of each network component. The intensity measure used in this article is peak ground acceleration (PGA). The simulation scheme used, explained in detail in [32], is briefly summarized hereafter.

After sampling the time of occurrence using a uniform distribution across the study period, the next step is to sample an earthquake magnitude (Mw) and hypocentral location (latitude, longitude, and depth) from an earthquake recurrence model, which was calibrated using a catalogue of historical earthquakes in the region [33]. The model divided the studied region into different seismic zones, and calibrated their seismic recurrences using their particular historical seismic data in order to capture differences in earthquake productivity. The sampled earthquake is then used to feed a ground-motion prediction model (GMPM), which estimates the PGA at a site given an earthquake magnitude, source-to-site distance, and other earthquake and site variables (e.g., focal depth and local soil conditions). The GMPM used here is specific for subduction-type earthquakes [34]. Moreover, since electric power systems are spatially distributed, the sampled intensities should be spatially correlated. This correlation is strong for sites that are close to each other and decays with site separation. The spatial correlation structure used in this article is the one developed by Jayaram and Baker [35].

The methodology also uses importance sampling in the generation of earthquake scenarios to improve efficiency. This variance reduction technique [5] is used to sample earthquake magnitudes with a uniform distribution instead of the original truncated exponential distribution, derived from the Gutenberg–Richter law [36], in order to increase the number of high magnitude scenarios, which contribute more to the overall seismic risk assessment.

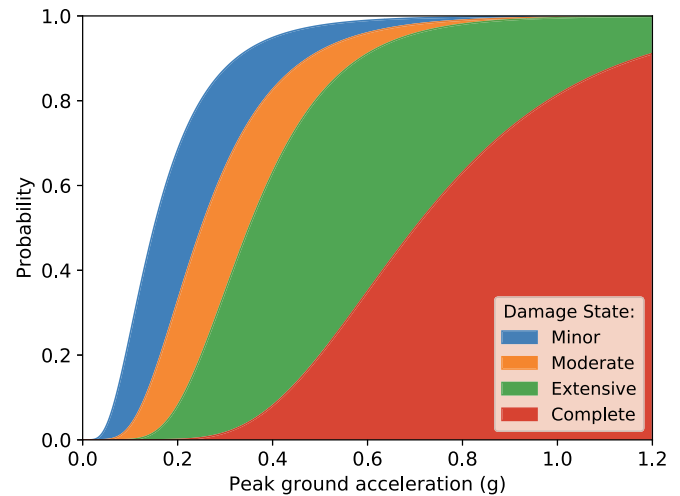


Fig. 3. Set of fragility curves for an anchored substation of medium voltage obtained from the Hazus software [38].

TABLE I
NETWORK COMPONENTS MODELED AS VULNERABLE

Vulnerable components	Classification
Substations	Anchored medium voltage (150 to 350 kV)
	Anchored low voltage (34.5 to 150 kV)
Thermal power plants	Anchored large capacity (≥ 200 MW)
	Anchored small capacity (< 200 MW)

2) Stage 2. Component Vulnerability: The aim of the second stage is to determine the damage state of each vulnerable component. This is achieved by using fragility curves, which express the probability of system components reaching different damage states conditioned to a PGA (as shown in Fig. 3). Fragility curves rest on structural analyses or empirical data and are usually represented by lognormal distributions; this characterization addresses uncertainties in the earthquake demand and the properties of the component under stress.

As shown in Table I, the electrical components modeled as vulnerable are substations and thermal power plants. Circuit towers, hydro plants, and solar photovoltaic plants are considered invulnerable since past experience in Chile shows that they have resisted well to seismic events [37], and the same is assumed for wind parks. Moreover, for the case study, in 2016, variable renewable sources represented a low capacity share (10%) compared to thermal plants (90%). Each vulnerable component is associated with a particular set of fragility curves, taken from the technical manual of the Hazus software [38]. All facilities were considered as “anchored” due to the similarities with the Chilean code.

The selected fragility curves are used to assign one of five different damage states to each component: none, minor, moderate, extensive, or complete. Damage states are modeled differently

for each type of vulnerable component identified, similarly as [38]. Substations with minor/moderate/extensive and complete damage states were assumed to have probabilities of disconnecting adjacent generators and circuits of 5%/40%/70% and 100%, respectively. Given a substation with disconnection probability p , the connection state of each adjacent element is determined from independent Bernoulli trials (i.e., experiments with only two random outcomes) with probability p . Power plants with any damage are disconnected from the system until restored.

3) *Stage 3. System Operation:* The uncertain time of the event strike is critical, because the time sets the demand level, generation maintenance and construction schedule, reserves deployed, variable renewable generation profiles, and online generation scheduled by the unit commitment. To represent this uncertainty, the model considers the actual operation data of 2016 published by the Chilean Independent System Operator (ISO) [39] for the hour sampled in Stage 1 as the starting condition.

Then, an hourly operation is performed based on a bespoke dc optimal power flow (dc-OPF) linear model at every hour until infrastructure is recovered. The aim is to minimize the ENS hour by hour while several components may be unavailable (unavailability represented by binary status constants u_g^t and u_l^t). The decision variables of the problem are power generated by each generation unit g (P_g), voltage angles of each node k (θ_k), network power flows ($f_l^{\mathcal{N}_1(l), \mathcal{N}_2(l)}$), and load shed at each node (LS_k). The problem solved for every scenario $s \in \mathcal{S}$ and hour $t \in \mathcal{T}$ is described by

$$\min \left\{ \sum_{g \in \mathcal{G}} P_g \times \Delta t \times \pi_g + \sum_{k \in \mathcal{N}} LS_k \times \Delta t \times M \right\} \quad (3)$$

subject to

$$\sum_{g \in \mathcal{G}(k)} P_g + LS_k - D_k + \sum_{l \in \mathcal{L}} f_l^{\mathcal{N}_1(l), k} - \sum_{l \in \mathcal{L}} f_l^{k, \mathcal{N}_2(l)} = 0 \quad \forall k \in \mathcal{N} \quad (4)$$

$$0 \leq P_g \leq \bar{P}_g \times u_g^t \quad \forall g \in \mathcal{G} \quad (5)$$

$$-u_l^t \times \bar{f}_l^{\mathcal{N}_1(l), \mathcal{N}_2(l)} \leq f_l^{\mathcal{N}_1(l), \mathcal{N}_2(l)} \leq \bar{f}_l^{\mathcal{N}_1(l), \mathcal{N}_2(l)} \times u_l^t \quad \forall l \in \mathcal{L} \quad (6)$$

$$f_l^{\mathcal{N}_1(l), \mathcal{N}_2(l)} = \frac{S_0}{x_l} \times (\theta_{\mathcal{N}_1(l)} - \theta_{\mathcal{N}_2(l)}) \times u_l^t \quad \forall l \in \mathcal{L} \quad (7)$$

$$0 \leq LS_k \leq D_k \quad \forall k \in \mathcal{N} \quad (8)$$

$$\theta_{k \neq \text{ref}} \text{ free} \quad \forall k \in \mathcal{N} \quad (9)$$

$$\theta_{\text{ref}} = 0 \quad \forall \text{ref} \in \{\text{unique node per system island}\}. \quad (10)$$

The objective function (3) is to minimize generation costs and a sufficiently large cost of ENS, subject to: real power balance for each node k (4); power production constraints for each generator subject to their availability (5); real power thermal constraints for each circuit (6); relation between circuit power flows and node voltage angles (7); constrain of LS to local demand (8); and nodal voltage angles as free variables (9), except for reference buses (10).

TABLE II
RECOVERY PARAMETERS (NORMAL DISTRIBUTIONS)

Components	Damage state	μ (days)	σ (days)
Substations	Minor	1.0	0.5
	Moderate	3.0	1.5
	Extensive	7.0	3.5
	Complete	30.0	15.0
Thermal power plants	Minor	0.5	0.1
	Moderate	3.6	3.6
	Extensive	22.0	21.0
	Complete	65.0	30.0

The hourly binary status constants, u_g^t and u_l^t , are determined before running each hourly optimization model starting from the 2016 operation data, which include component maintenance, construction schedule, and unit-commitment starting conditions; and then considering the sampled component outages, black-start capabilities of the system island, and start-up time requirements, as explained next.

Given that $M \gg \pi_g$, the optimal operation of the system can be neglected in comparison to the cost of ENS; hence, the model optimizes the operation to minimize the LS. Moreover, the information that feeds the risk measures is only the ENS valued at VoLL.

It is important to acknowledge that the model is based on a multiperiod dc model, which has several shortcomings, particularly during extreme conditions, such as earthquakes and islanded operation due to, amongst others, the nonconsideration of dynamic and intertemporal constraints. The rationale of using the described model is due to its linearity and the possibility to run a considerable number of scenarios in a manageable time. Further discussion and comparison of the impacts of using different models in the context of seismic impacts on electric power systems can be found in [40], where the authors conclude that, between steady-state models, the dc model nearly always underestimates the consequences compared to the ac model.

4) *Stage 4. System Restoration:* The number of hours simulated depends on the complete recovery time of the system. Depending on the type of component classification and its damage state determined in Stage 2, the component downtimes are sampled from normal distributions with the parameters estimated by Hazus [38], reproduced in Table II. Components that fulfill their restoration time become available after they also fulfill their start-up times. Also, power plants that were not damaged, but were offline at the time of the event, become available only after their start-up times. Finally, given that multiple failures arising from the scenarios can induce system islands [41], black-start capabilities of islands are checked before being able to restart operations.

B. Risk Quantification and Uncertainty Management

To incorporate the diverse uncertainties in the different stages, the risk assessment methodology considers several random variables as summarized in Table III.

TABLE III
STOCHASTIC VARIABLES INCORPORATED

Variable	Description
Earthquake magnitude	Sampled from a uniform distribution instead of natural Gutenberg-Richter recurrence model (importance sampling)
Earthquake time of occurrence	Sampled uniformly from 2016 data with an hourly resolution.
Originating seismic source	Selected from the sources of Chile.
Epicentral location	Longitude, latitude, and depth within the selected originating source.
Peak Ground Acceleration (PGA)	Determined by a GMPM at the locations of all components.
Component damages states	Determined by using the respective PGAs and fragility curves.
Substations adjacent connections (lines and power plants)	Sampled from Bernoulli distribution. The disconnection probability depends on the damage state of the associated substation.
Component downtimes	Determined using normal distributions that depend on damage states.

Monte Carlo simulations are used to handle this significant stochasticity and compute the overall seismic risk of the system using the results from all scenarios. However, a drawback is the substantial number of simulations required to achieve acceptable confidence on the results, which is computationally expensive. Hence, as aforementioned, importance sampling is used to increase the frequency of high-magnitude earthquakes since it has shown to improve the convergence significantly [32].

The risk assessment methodology, described in more detail in [32], combines the system losses in terms of ENS and IC across all scenarios, in order to estimate the mean annual frequency of events exceeding different values of these losses. This mean annual frequency curve is then used to compute the accumulated losses of the system for a given time window of length z (A_z). This random variable represents the sum of losses of all events that occur in the time window, and its probability distribution can be calculated using an analytical or simulation-based procedure, as presented in [42]. This assessment assumes that earthquake events occurrences follow a homogeneous Poisson stochastic process, a common assumption in seismic hazard and risk analysis.

The seismic risk of the system is then quantified with three different risk measures, namely, the expected loss within a year timeframe, EAL; the loss with an α -probability of exceedance in a time window z , $\text{VaR}^z(\alpha)$; and the expected loss in the worst $\alpha \times 100\%$ of cases in a time window z , $\text{CVaR}^z(\alpha)$ [43]. All measures can be computed directly from variable A_z as

$$\text{EAL} = E[A_{1 \text{ year}}] \quad (11)$$

$$\text{VaR}^z(\alpha) = F_B^{-1}(1 - \alpha) \quad (12)$$

$$\text{CVaR}^z(\alpha) = \frac{1}{\alpha} \int_0^\alpha \text{VaR}(\xi) d\xi \quad (13)$$

where $E[\cdot]$ is a variable expected value; $B = A_z$; and F_B is its associated cumulative distribution function (CDF).

C. Criticality Assessment

Importance measures determine the relative importance of a component with respect to other components of a system. Whereas previous work has based the system enhancement strategy under seismic action with a subjective view ([14] because the “identification of both the critical nodes and minimum paths requires some (subjective) engineering judgment”), this article, based on the Fussell–Vesely (FV) importance measure [44], objectively quantifies importance as the relative reduction of losses of a system when the component under study is assumed invulnerable. The FV-variant for component i ($\text{FV}v_i$), expressed as percentage, is calculated from a risk measure of the system under the default configuration (RM_0) and the same risk measure assuming component i invulnerable (RM_i), as expressed in (14). FV-variant may be defined based on any metric (e.g., ENS and IC) and risk measure (e.g., EAL, VaR, and CVaR) as follows:

$$\text{FV}v_i = \frac{\text{RM}_0 - \text{RM}_i}{\text{RM}_0} \times 100\%. \quad (14)$$

As stated by [31], importance measures are fundamental in addressing complex reliability problems because they provide insight on system structures and constitutive components. The FV-variant presented here is an improved importance measure in various aspects, which are listed in Section I.

Since electric power systems are usually managed to satisfy $N-1$ contingencies, which means that the failure of any one component should not result in any ENS, importance measures assuming single components invulnerable would not produce conclusive results. However, since the seismic scenarios studied here also produce multiple failures, it is adequate to work with single invulnerable components.

III. STUDY CASE: NORTHERN CHILEAN ELECTRIC POWER SYSTEM (SING)

The region under analysis is a subduction zone controlled by the convergence of the Nazca and South American tectonic plates that overlap at rate of about 7 cm/year. The last important earthquakes were the 1868 Arica $M_w 9.0$, the 1877 Iquique $M_w 8.8$ (which produced a tsunami with wave heights up to 17 m), the 1995 Antofagasta $M_w 8.0$, the 2007 Tocopilla $M_w 7.7$, and the 2014 Iquique $M_w 8.2$. However, the region still has a seismic gap that may generate a significant event in the near future.

The case study is a close representation of the Northern Interconnected System (SING) as it was at the end of 2016, which covered 25% of the national continental territory, though only 7% of its population. In 2016, the electricity consumption was 17.2 TWh, from which the mining industry demanded 13 TWh, industrial consumers 2.3 TWh, and residential users from distribution networks only 1.9 TWh [39]. Hence, the model does not consider detailed distribution networks in order to increase

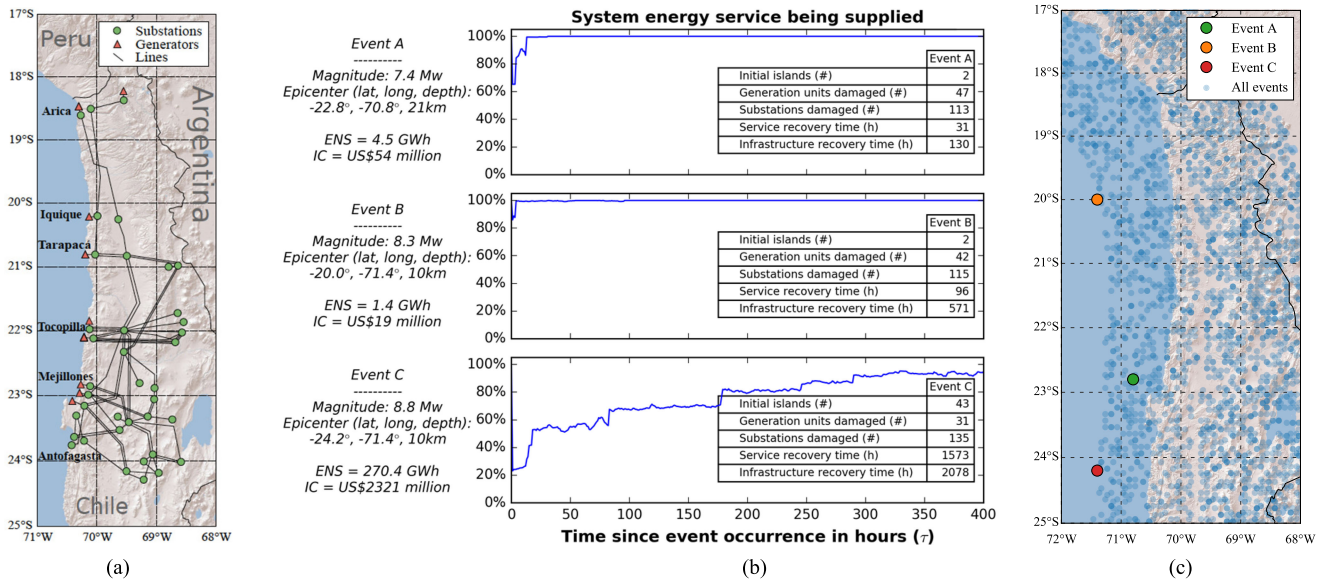


Fig. 4. (a) Map of the Northern Chilean simplified electric power network. (b) Evolution of energy being supplied for three simulated scenarios. (c) Scenario epicenters considered.

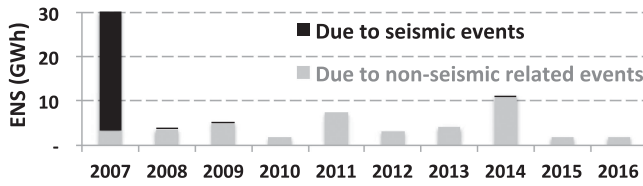


Fig. 5. Historical annual energy not supplied (ENS) at SING.

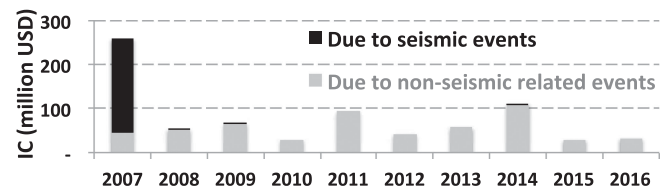


Fig. 6. Historical annual interruption costs (IC) at SING.

the computational efficiency, but can easily be extended with more detailed data.

The SING network is shown in Fig. 4(a) and comprises 101 substations, 150 circuits, and 34 power plants. Most of the power plants are located on the coast and are modeled as 64 independent generation units that add up to 5.1 GW of net capacity (i.e., discounting selfconsumption). Of these units, 51 are dispatchable thermal units, characterized by variable costs, start-up times, and black-start capabilities, which account for 4.6 GW (90% of the total net capacity). The other 13 units are solar, wind, and small run of river, which account for 0.5 GW, are considered invulnerable to seismic impact, and are characterized by their actual 2016 hourly generation profiles. Further 13 generation units were under construction and are considered available from their operation start date onward. More details of the system are given in Tables VII–IX of the appendix.

Figs. 5 and 6 show historical data from the SING ISO for the decade between 2007 and 2016 of all failures registered. Nonseismic-related events, such as demand or generation sudden variability, lines tripping due to temperature conditions, endogenous substation's component failures due to their utilization and life cycle, etc., are depicted in light grey. The SING suffered annual losses of 7 GWh on average, accounting for US\$77 million. However, solely in the year 2007, SING had losses of

TABLE IV
INTERRUPTION COST PARAMETERS (US\$/MWH)

Type of consumer	First 20 min.	20 min < t < 60 min.	60 min < t < 240 min	After 240 min.
Mining/Industry	50,182	14,932	12,785	8,323
Residential	9,708	9,708	9,708	9,708

US\$260 million, mostly due to seismic events, which highlights the need for considering and planning against high-impact, low-probability events.

VoLL_k^t used here is determined with interruption cost parameters from a study delivered to the SING ISO in 2016, which are presented in Table IV, with a foreign exchange rate of 670 (CLP/USD)^{Jan-2017}. The unserved energy is valued differently by type of consumers; thus, mining/industry cost parameters are nonidentical and change with time due to their contingency and back-up plans. During the first hour and in substations shared by both type of consumers, consumption-weighted average of the cost parameters is used to determine VoLL_k^t for every substation $k \in \mathcal{N}$ and hour $t \in \mathcal{T}$. With the required data, more differentiation can be easily considered (e.g., government

TABLE V
BASE CASE RESULTS OF RISK MEASURES

Time window (z):	1 year	10 years	20 years	50 years
Energy not supplied (GWh)	VaR	56	491	772
	CVaR	195	732	1047
Interruption costs (million USD)	VaR	482	3462	4598
	CVaR	1634	5160	6312

buildings, hospitals, banking district, water supply, and other critical infrastructure).

IV. RESULTS

A. Base Case

A total of 90 000 earthquake scenarios were considered in the analysis, with epicenters shown in Fig. 4(c). The scenarios were first applied to the system with all components considered vulnerable, as in reality, which is referred to as the base case. Fig. 4(b) presents three of the simulated scenarios in terms of their energy being supplied over time. It can be seen that a higher earthquake magnitude does not necessarily produce higher losses, since there are several other variables to consider (see Table III). Besides ENS and IC, each simulation identifies damage states for each component, a recovery time for the service and for the complete restoration of the infrastructure, the reconnection evolution of network islands, amongst others, which can be further analyzed.

The simulations for the base case resulted in an expected annual ENS of 12.7 GWh, accounting for an expected annual IC of US\$109.7 million (EAL).

Although the model objective is to calculate potential future impacts and not historical impacts, the resulting expected annual losses are of the same order of magnitude of the historical data presented in Figs. 5 and 6. In particular, the expected annual ENS and IC due to seismic events are of the same order of magnitude as the averages of the last decade, which were approximately 3 GWh and US\$22 million, respectively.

Table V presents the risk measures VaR and CVaR of the ENS and IC variables for different time windows and $\alpha = 0.05$. For IC, a real discount rate of 4% to bring costs to present value was considered.

The risk measures presented here are just examples of what may be used by decision makers. Further results, presented as CDF, are shown in Fig. 7 as accumulated interruption costs across time windows of 10, 20, and 50 years.

B. Component Criticality Ranking

In order to analyze the criticality of each vulnerable component, i.e., the 101 substations and 51 generation units, the same simulations performed for the base case were repeated for each of the 152 cases in which each vulnerable component was independently considered invulnerable. Criticality was then

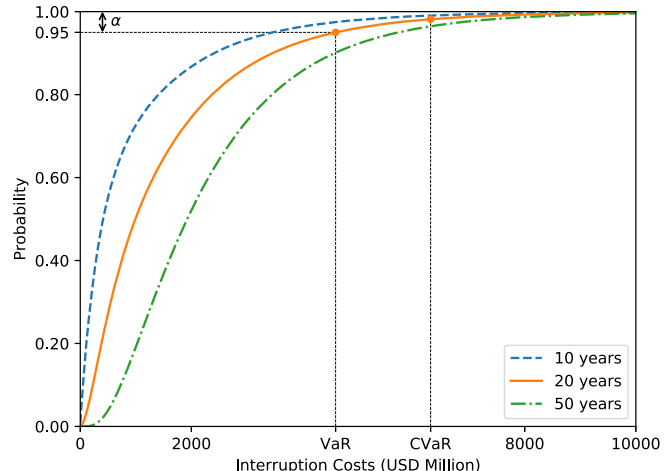


Fig. 7. CDF of the accumulated interruption costs for different time windows. VaR and CVaR are calculated with a time window of 20 years and $\alpha = 0.05$.

assessed with (14) and using three IC risk measures, namely, EAL, $\text{VaR}^{20\text{years}}$, and $\text{CVaR}^{20\text{years}}$, with $\alpha = 5\%$. The resulting criticality values for the 10 most critical substations and 10 most critical generation units according to EAL are shown in Fig. 8. Initially, it was thought that the criticality ranking of components could notably change depending on the risk measure considered. However, the criticality values and resulting rankings using the three risk measures are fairly similar. Some exceptions of this were substations ranked 18th, 11th, and 14th based on $\text{VaR}^{20\text{years}}$ and 20th, 13th, and 16th based on $\text{CVaR}^{20\text{years}}$, which moved to the 8th, 9th, and 10th place as seen in Fig. 8(a).

Focusing on EAL as the risk measure, seven substations and two generation units resulted in improvements of more than 3%, as stated in Fig. 8. Consequently, it may be concluded that a selective retrofit program that focuses on these components may be justifiable. This is also reflected in Fig. 9, where component importance is shown to be heterogeneously distributed across the system.

An interesting result from the 152 cases of 90 000 scenarios simulated was that 0.018% of these scenarios had more ENS than the base case. This counter intuitive result was due to topology constraints, where lines of substations considered invulnerable secured more transportation capacity, as from (6), but along with more flow constraints, as from (7), which worsened the simulation results. This reflects the importance, in general, of considering corrective control actions, particularly line switching. Nevertheless, given the low number of scenarios where this occurred, it was of low significance for the outcomes pursued in this article.

C. Relative Importance of Various Factors

To analyze the most important factors that determine component criticality, a linear correlation was assessed by calculating the Pearson correlation coefficient (ρ) between the EAL of ENS and several potential explanatory properties of the associated invulnerable component, which are shown in Table VI. When

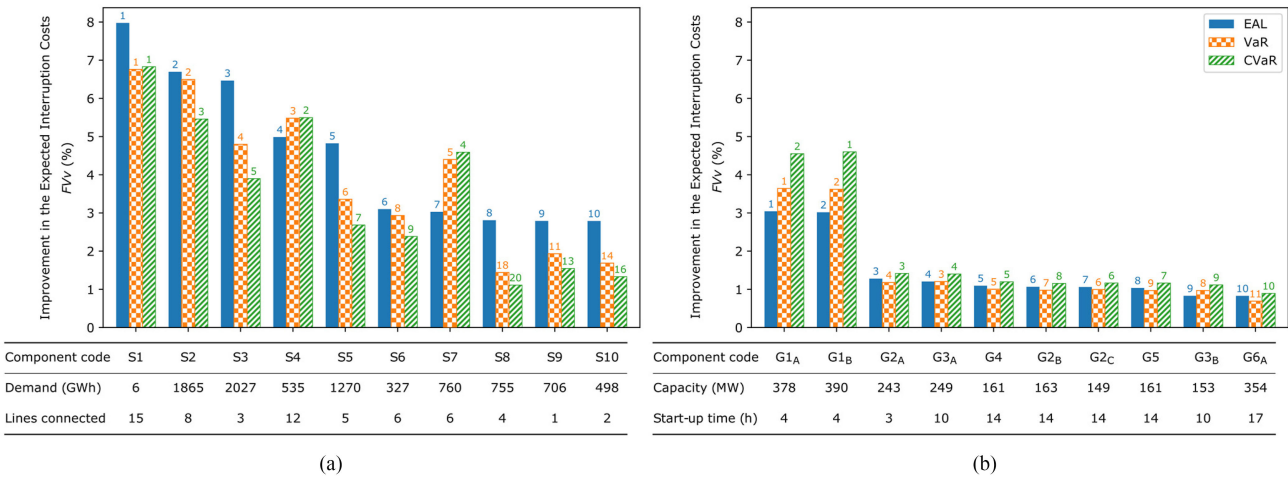


Fig. 8. Criticality of the most critical components using EAL (blue bars), VaR²⁰ years (orange bars), and CVaR²⁰ years (green bars). Numbers on top of bars correspond to the ranking associated to each component in terms of different risk measures. (a) Substations, S1–S10. (b) Generation units, G1_A–G6_A.

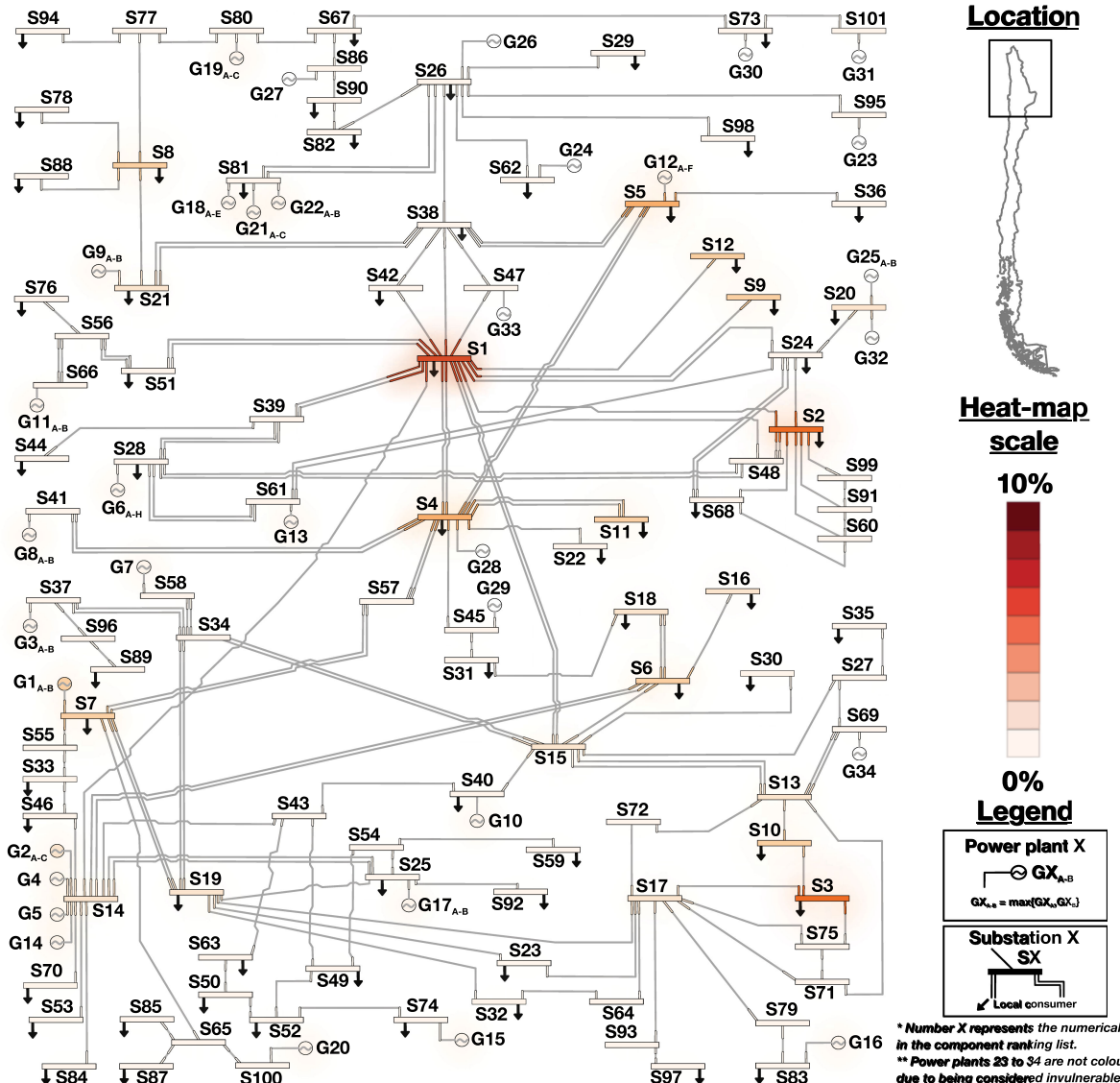


Fig. 9. Electrical diagram of the network and criticality heat-map based on FVv (%) in terms of the expected annual loss of interruption costs.

TABLE VI
PEARSON CORRELATION COEFFICIENT BETWEEN EXPECTED ANNUAL LOSS OF ENS AND VARIOUS VARIABLES

Component\Property	Annual demand	Number of circuit connections	Net generation capacity connected	Expected annual PGA per event
Substations	0.74	0.60	0.11	0.39
Component\Property	Net capacity	Start-up time	Number of online hours	Expected annual PGA per event
Thermal plants	0.77	0.28	0.45	-0.06

the value of ρ is close to zero, the explanatory factor is considered not relevant. Otherwise, the higher the value of ρ , the explanatory factor is considered to contribute more to component criticality.

The results show that the most and least contributing factors analyzed for substation criticality are local demand and generation capacity connected, respectively. The second most important factor is the number of connections, which implies that the topology of the network is crucial and a simplification of the topology may misrepresent the problem. The thermal power plant results show that the most important factor for their criticality is their generation capacity, followed by the number of hours they are online during the year. Finally, as a hazard exposure characterization, the expected annual PGA per event shows no significance for the criticality of thermal plants since they are mostly in the coast and hence exposed to similar hazard intensity.

V. CONCLUSION, LIMITATIONS, AND FUTURE WORK

Although the largest disasters capture most of the global attention, the cumulative effect of small- and medium-size events has an important impact on the economy. The novel risk and resilience assessment methodology presented here for electric power systems is able to incorporate all potential scenarios probabilistically while quantifying, with different risk measures, physical impacts (ENS) and economic impacts (IC) with time-dependent simulations. The proposed methodology is a step toward managing risk, rather than using preconceived scenarios.

For the study case, future expected annual interruption costs are estimated at approximately US\$110 million. This is the amount that Chile should set aside each year to cover future seismic losses in the SING due to unserved energy alone, whereas the average historical data per year of losses during a ten-year period is close to US\$22 million. The differences when comparing the results of the model with the historical data are theoretically explained by the fact that the historical data represent only one decade, which is a small time window compared to earthquake recurrences. The return period of earthquakes with magnitude greater than, say, 8.5 is roughly 100 years in the region. The differences may also be explained by some methodological biases. For example, the system was modeled as it stood in 2016, and hence, compared to historical data, ENS and IC may

be overestimated because Chile's hazard exposure has increased steadily over time due to a 3.8% compound annual growth rate of demand between 2007 and 2016.

Moreover, the results presented in this article are based on the specific assumptions and parameters used. For example, the damage model is based on the information proposed by the Hazus software [38], but could be changed appropriately. Nevertheless, these arbitrary selections do not affect the applicability of the methodology. Each of the model stages can be improved in accuracy by collecting more detailed information. For instance, by incorporating a detailed distribution-level model, modeling the microcomponents of power plants and substations, and considering the vulnerability of towers and renewable power plants. Other limitations are the nonconsideration of possible interdependencies with other critical infrastructure systems, the omission of cascading failures, and possible damage to power system protections. Furthermore, the assumption that the power system is required to provide the same energy as if there were no impact on consumers does not apply in real situations, as both residential and industrial/mining consumers are also impacted by the event, with a demand reduction as a result.

Although the presented assessment is based on several informed assumptions, the authors acknowledge that they are only estimations, which emphasizes the importance of using a probabilistic approach. Moreover, the results of the methodology are based not only on absolute terms, but also on relative component criticality rankings to prioritize and communicate results in a novel manner. Comparing and ranking alternatives using a theoretical consistent model may contribute to better understand the impact natural disasters on electric power systems.

Increasing the resilience of critical power infrastructure to high-impact, low-probability events through mitigation and adaptation measures is of enormous importance to keep the lights on. The outcomes of the analysis presented may be harnessed by several risk management actions. The quantitative assessment through various indicators can provide useful information for the electricity network planning phase (e.g., construction of new components and reduction of component restoration times), help test the effectiveness of possible structural actions (e.g., structural retrofit of components and new construction design standards), and support the creation of innovative finance instruments (e.g., pooled insurances and securitized debt). Moreover, criticality ranking can be a useful tool for component intervention prioritization in the preventive and recovery phase, and to inform stakeholders on the level of risk exposure and resilience of critical infrastructure.

Future work involves considering the effects of seismic aftershocks and tsunamis, considering system interdependencies with other critical infrastructure (as performed in [45]), including a superior ac operational model with intertemporal constraints and possible actions (e.g., reserves), and a more complex recovery model that considers human and resources optimization. Furthermore, as initiated by Romero *et al.* [13] and Nazemi *et al.* [46], distribution, transmission, and generation expansion planning models can be developed building on the risk and resilience methodology presented in this article.

APPENDIX

TABLE VII
GENERATION DATA

Gen. technology	Total net capacity (MW)	Power plants (#)	Gen. units (#)	Large capacity units (# \geq 200MW)	Small capacity units (# $<$ 200MW)
Coal	2,344	6	15	4	11
Gas	1,959	3	8	5	3
Oil	277	12	27	0	27
Solar	313	9	10	0	10
Wind	201	2	2	0	2
Hydro	11	1	1	0	1
Cogeneration	18	1	1	0	1
Total	5,121	34	64	9	55

TABLE VIII
SUBSTATIONS DATA

Substation classification	Number (#)
Medium voltage (150 to 350 kV)	59
Low voltage (34.5 to 150 kV)	42
Total	101

TABLE IX
LINES DATA

Lines voltages (kV)	Number (#)
220	97
110	31
100	11
66	12
34.5	4
Total	155

REFERENCES

- [1] UNISDR, *Global Assessment Report on Disaster Risk Reduction*. New York, NY, USA: United Nations, 2015.
- [2] M. Dilley *et al.*, *Natural Disaster Hotspots: A Global Risk Analysis*. Washington, DC, USA: World Bank Publ., 2015.
- [3] Financial Markets Commission of Chile. *Earthquake 2010: Analysis and Impact of the 27-F on the Insurance Market*. Santiago, Chile: SVS, Publ. 2012.
- [4] T. Aven, *Foundation of Risk Analysis*. Hoboken, NJ, USA: Wiley, 2003.
- [5] R. Billinton and W. Li, *Reliability Assessment of Electric Power Systems Using Monte Carlo Methods*. New York, NY, USA: Plenum Press, 1994.
- [6] J. He, L. Cheng, D. Kirschen, and Y. Sun, "Optimising the balance between security and economy on a probabilistic basis," in *IET Generation, Transmission Distribution*, vol. 4, no. 12, pp. 1275–1287.
- [7] J. McCalley, A. Fouad, V. Vittal, A. Irizarry-Rivera, B. Agrawal, and R. Farmer, "A risk-based security index for determining operating limits in stability-limited electric power systems," *IEEE Trans. Power Syst.*, vol. 12, no. 3, pp. 1210–1217, Aug. 1997.
- [8] J. McCalley, V. Vittal, and N. Abi-Samra, "Use of probabilistic risk in security assessment: A natural evolution," in *Proc. Int. Conf. Large High Voltage Elect. Syst., CIGRE Session*, Paris, 2000, pp. 1–10.
- [9] D. Kirschen, K. Bell, D. Nedic, D. Jayaweera, and R. Allan, "Computing the value of security," *IEEE Proc. Gener., Transmiss. Distrib.*, vol. 150, no. 6, pp. 673–678, Nov. 2003.
- [10] D. Kirschen, D. Jayaweera, D. Nedic, and R. Allan, "A probabilistic indicator of system stress," *IEEE Trans. Power Syst.*, vol. 19, no. 3, pp. 1650–1657, Aug. 2004.
- [11] D. Kirschen and D. Jayaweera, "Comparison of risk-based and deterministic security assessments," *IET Gener. Transmiss. Distrib.*, vol. 1, no. 4, pp. 527–533, Jul. 2007.
- [12] F. Capitanescu *et al.*, "State-of-the-art, challenges, and future trends in security constrained optimal power flow," *Elect. Power Syst. Res.*, vol. 81, no. 8, pp. 1731–1741, 2011.
- [13] N. Romero, L. Nozick, I. Dobson, N. Xu, and D. Jones, "Transmission and generation expansion to mitigate seismic risk," *IEEE Trans. Power Syst.*, vol. 28, no. 4, pp. 3692–3701, Nov. 2013.
- [14] I. Vanzi, "Structural upgrading strategy for electric power networks under seismic action," *Earthq. Eng. Struct. Dyn.*, vol. 29, pp. 1053–1073, 2000.
- [15] K. Pitilakis, H. Crowley, and A. Kaynia, Eds, *SYNER-G: System Seismic Vulnerability and Risk Assessment of Complex Urban, Utility, Lifeline Systems and Critical Facilities*. Berlin, Germany: Springer, 2010, ch. 10, pp. 301–330.
- [16] J. Buriticá, M. Sánchez-Silva, and S. Tesfamariam, "A hierarchy-based approach to seismic vulnerability assessment of bulk power systems," *Struct. Infrastruct. Eng.*, vol. 11, no. 10, pp. 1352–1368, 2015.
- [17] S. Espinoza *et al.*, "Seismic resilience assessment and adaptation of the Northern Chilean Power System," in *Proc. IEEE Power Energy Soc. General Meeting Conf.*, Chicago, FL, USA, 2017, pp. 1–5.
- [18] D. Henry and J. E. Ramirez-Marquez, "Generic metrics and quantitative approaches for system resilience as function of time," *Rel. Eng. Syst. Saf.*, vol. 99, pp. 114–122, 2012.
- [19] Y. Wang, C. Chen, J. Wang, and R. Baldick, "Research on resilience of power systems under natural disasters-A review," *IEEE Trans. Power Syst.*, vol. 31, no. 2, pp. 1604–1613, Mar. 2016.
- [20] M. Ouyang and L. Dueñas-Osorio, "Multi-dimensional hurricane resilience assessment of electric power systems," *Struct. Saf.*, vol. 48, pp. 15–24, 2014.
- [21] M. Panteli and P. Mancarella, "The grid: Stronger, bigger, smarter?" *IEEE Power Energy Mag.*, vol. 13, no. 3, pp. 58–66, May/Jun. 2015.
- [22] S. Espinoza, M. Panteli, P. Mancarella, and H. Rudnick, "Multi-phase assessment and adaption of power systems resilience to natural hazards," *Elect. Power Syst. Res.*, vol. 136, pp. 352–361, 2016.
- [23] R. Paredes, and L. Dueñas-Osorio, "A time-dependent seismic resilience analysis approach for networked lifelines," in *Proc. 12th Conf. Appl. Statist. Probability Civil Eng.*, Vancouver, BC, Canada, 2015, pp. 1–8.
- [24] M. Shinozuka, X. Dong, T. Chen, and X. Kin, "Seismic performance of electric transmission network under component failures," *Earthq. Eng. Struct. Dyn.*, vol. 36, pp. 224–227, 2007.
- [25] Z. Birnbaum, "On the importance of different components in a multi-component system," *Multivariate Anal.*, vol. 11, pp. 1–20, 1969.
- [26] J. Li, L. Dueñas-Osorio, C. Chen, and C. Shi, "AC power flow importance measures considering multi-element failures," *Rel. Eng. Syst. Saf.*, vol. 160, pp. 89–97, 2017.
- [27] M. Panteli, C. Pickering, S. Wilkinson, R. Dawson, and P. Mancarella, "Power system resilience to extreme weather: Fragility modelling, probabilistic impact assessment, and adaptation measures," *IEEE Trans. Power Syst.*, vol. 32, no. 5, pp. 3747–3757, Sep. 2017.
- [28] G. Fu *et al.*, "Integrated approach to assess the resilience of future electricity infrastructure networks to climate hazards," *IEEE Syst. J.*, vol. 12, no. 4, pp. 3169–3180, Dec. 2017.
- [29] M. Bessani *et al.*, "Probabilistic assessment of power distribution systems resilience under extreme weather," *IEEE Syst. J.*, vol. 13, no. 2, pp. 1747–1756, Jun. 2019.
- [30] M. Panteli and P. Mancarella, "Modeling and evaluating the resilience of critical electrical power infrastructure to extreme weather events," *IEEE Syst. J.*, vol. 11, no. 3, pp. 1733–1742, Sep. 2017.
- [31] W. Kuo and X. Zhu, "Some recent advances on importance measure reliability," *IEEE Trans. Rel.*, vol. 61, no. 2, pp. 344–360, Jun. 2012.
- [32] A. Poulos *et al.*, "Seismic risk assessment of spatially distributed electric power systems," in *Proc. 16th W. Conf. Earthq. Eng.*, Santiago, Chile, 2017, pp. 1–11.

- [33] A. Poulos *et al.*, “An updated recurrence model for Chilean subduction seismicity and statistical validation of its Poisson nature,” *Bull. Seismol. Soc. Amer.*, vol. 109, no. 1, pp. 66–74, 2019.
- [34] N. Abrahamson *et al.*, “BC Hydro ground motion prediction equations for subduction earthquakes,” *Earthq. Spectra*, vol. 32, no. 1, pp. 23–44, 2016.
- [35] N. Jayaram and J. Baker, “Correlation model for spatially distributed ground-motion intensities,” *Earthq. Eng. Struct. Dyn.*, vol. 38, pp. 1687–1708, 2010.
- [36] Gutenberg and C. Richter, “Frequency of earthquakes in California,” *Bull. Seismol. Soc. Amer.*, 34, no. 4, pp. 185–188, 1944.
- [37] H. Rudnick *et al.*, “Disaster management,” *IEEE Power Energy Mag.*, vol. 9, no. 2, pp. 37–45, Mar./Apr. 2011.
- [38] Federal Emergency Management Agency, *Hazus -MH MR5: Technical Manual*. Washington, DC, USA, 2015.
- [39] CDEC-SING (ISO). Retiro de Energía a Clientes 2016. [Online]. Available: goo.gl/L0vLm7, Accessed: Mar. 21, 2017.
- [40] S. LaRocca, J. Johansson, H. Hassel, and S. Guikema, “Topological performance measures as surrogates for physical flow models for risk and vulnerability analysis for electric power systems,” *Risk Anal.*, vol. 35, no. 4, pp. 608–623, 2015.
- [41] J. Quirós-Tortós, P. Demetriou, M. Panteli, E. Kyriakides, and V. Terzija, “Intentional controlled islanding and risk assessment: A unified framework,” *IEEE Syst. J.*, vol. 12, no. 4, pp. 3637–3648, Dec. 2018.
- [42] A. Poulos *et al.*, “Earthquake risk assessment of buildings accounting for human evacuation,” *Earthq. Eng. Struct. Dyn.*, vol. 46, no. 4, pp. 561–583, 2017.
- [43] R. Rockafellar, and S. Uryasev, “Optimization of conditional value-at-risk,” *J. Risk*, vol. 2, no. 3, pp. 21–41, 2000.
- [44] W. Vesely, T. Davis, R. Denning, and N. Saltos, “Measures of risk importance and their applications,” US Nucl. Regulatory Commission, Rockville, MD, USA, Tech. Rep. NUREG/CR-3385, 1983.
- [45] Q. Zou and S. Chen, “Enhancing resilience of interdependent traffic-electric power system,” *Rel. Eng. Syst. Saf.*, vol. 191, pp. 1–18, 2019.
- [46] M. Nazemi, M. Moeini-Aghaie, M. Fotuhi-Firuzabad, and P. Dehghanian, “Energy storage planning for enhanced resilience of power distribution networks against earthquakes,” *IEEE Trans. Sustain. Energy*, vol. 11, no. 2, pp. 795–806, Dec. 2019.



Sebastián Espinoza (Member, IEEE) received the Industrial Electrical Engineer degree and the M.Sc. degree in electrical engineering from the Pontificia Universidad Católica de Chile (PUC), Santiago, Chile, in 2015. He is currently working toward the master’s degree in business administration and the master’s degree in public policy with Stanford University, Stanford, CA, USA, as a Knight-Hennessy Scholar.

He was a Researcher and Lecturer with PUC and a Chief Strategy Officer with the renewable energy company Valhalla, Santiago, Chile, until 2019. His research interests include risk and resilience analysis, electricity markets design, climate change impact, natural disasters, and countries’ energy and economic development.



Alan Poulos received the M.Sc. degree in civil engineering from the Pontificia Universidad Católica de Chile, Santiago, Chile, in 2014. He is currently working toward the Ph.D. degree in civil and environmental engineering with Stanford University, Stanford, CA, USA.

He was a Researcher with the National Research Center for Integrated Natural Disaster Management, Santiago, Chile, and an R&D engineer with Sirve S.A., Santiago, Chile. His research interests include earthquake engineering, probabilistic seismic hazard analysis, and seismic risk and resilience of buildings and spatially distributed systems.



Hugh Rudnick (Fellow, IEEE) received the electrical engineering degree from Universidad de Chile, Santiago, Chile, in 1974. He received the M.Sc. and Ph.D. degrees in electrical engineering from the Victoria University of Manchester, Manchester, U.K., in 1977 and 1982, respectively.

He is currently an Emeritus Professor of Engineering with the Pontificia Universidad Católica de Chile, Santiago, Chile, and the Director of Systep Engineering Consultants, Santiago, Chile. His research interests include the market and economic aspects of

the electrical power sector.

Dr. Rudnick is a Foreign Member of the National Academy of Engineering, Washington, DC, USA.



Juan Carlos de la Llera graduated from the Pontificia Universidad Católica de Chile (PUC), Santiago, Chile, in 1985, majoring in structural engineering. He received the M.Sc. and Ph.D. degrees in civil engineering from UC Berkeley, Berkeley, CA, USA, in 1990 and 1994, respectively.

He has been the Dean of the Faculty of Engineering, PUC, for the past ten years. He is currently the PI of the risk and resilience cluster of the National Center for the Integrated Management of Natural Disasters, Chile, CIGIDEN. He recently directed a national committee for the strategy of the country in Disaster Resilience, and is currently leading a new public institute for R&D in Resilience in Chile. He was also part of the group proposing a new Ministry of Science, Technology, and Innovation for Chile. His research interests include seismic protection of structures and systems, seismic risk analysis, and nonlinear structural dynamics.

Dr. de la Llera was the recipient of the Endeavor Entrepreneur Award of the year, in San Francisco, California, in 2011, for the successful performance of his seismic protection technology in the 2010 Chile earthquake, and the Innovation Trajectory Award given by Avonni in 2017, besides his awards as a researcher and academician.



Mathaios Panteli (Senior Member, IEEE) received the M.Eng. degree from the Aristotle University of Thessaloniki, Thessaloniki, Greece, in 2009, and the Ph.D. degree in electrical power engineering from The University of Manchester, Manchester, U.K., in 2013.

He is currently an Assistant Professor with the Power and Energy Division, The University of Manchester, Manchester, U.K. His main research interests include the analysis and prevention of blackouts, risk and resilience assessment of power systems, and integrated modeling of codependent critical infrastructures.

Dr. Panteli is an IET Chartered Engineer (CEng), the Co-Chair of the CIGRE WG C4.47 “Power System Resilience,” and an Active Member of multiple IEEE working groups on power grid resilience.



Pierluigi Mancarella (Senior Member, IEEE) received the M.Sc. and Ph.D. degrees in electrical energy systems from the Politecnico di Torino, Torino, Italy, in 2002 and 2006, respectively.

He is currently a Chair Professor of Electrical Power Systems with The University of Melbourne, Melbourne, VIC, Australia, and a Professor of Smart Energy Systems with The University of Manchester, Manchester, U.K. His research interests include multienergy systems, power system integration of low-carbon technologies, network planning under uncertainty, and risk and resilience of smart grids.

Dr. Mancarella is an Editor of the IEEE TRANSACTIONS ON POWER SYSTEMS and the IEEE TRANSACTIONS ON SMART GRID, an Associate Editor of the IEEE SYSTEMS JOURNAL, and an IEEE Power and Energy Society Distinguished Lecturer.